Thin-Film Electrodes Based on Two-Dimensional Nanomaterials for Neural Interfaces

Shaikh Nayeem Faisal[a], *Francesca Iacopi*[a, b*]

[a] University of Technology Sydney, School of Electrical and Data Engineering, Faculty of Engineering and Information Technology, Ultimo NSW, 2007, Australia.

[b]Australian Research Council Centre of Excellence for Transformative Meta-Optical Systems, University of Technology Sydney, Ultimo NSW, 2007, Australia.

E-mail: francesca.iacopi@uts.edu.au

KEYWORDS: 2D nanomaterials, graphene, thin-film sensors, neural interfaces, electroencephalography.

ABSTRACT: The detection and monitoring of neural signals is a fast -advancing area of research expected to impact a broad range of advanced applications, from healthcare to brain-machine and even brain-to-brain communications. Two-dimensional layered materials such as graphene, MXenes, and transition metal dichalcogenides, could lead to the development of superior and ultra-thin thin-film electrodes for neural interfaces thanks to their atomic thickness, high-conductivity properties, and potential to combine additional functionalities. This review focuses on the recent advancement of 2D materials-based thin-film sensors for the monitoring of biophysiological signals using invasive and non-invasive approaches.

1. INTRODUCTION

With the rapid recent progress of Neuroscience, there is a corresponding need to advance the way the biopotentials of the neurons in the human brain can be accurately sampled, assessed and decoded. This key function is carried out through specifically tailored sensors also called neural interfaces. The continued advancement of Neuroscience, as well as that of a number of applications revolving around efficient healthcare and health monitoring, in addition to the realisation of technologies based on brain-machine interaction, all rely on the development of highly accurate and biocompatible neural interfaces. Neural interfaces are a class of devices

that interact with the nervous system. They are electronic sensing devices interfacing with the brain or the nervous system in general which can be placed either externally (wearables) or inside (implants) the body to record or stimulate neural activity. [1, 2]

Recent progress in (nano)materials, including their synthesis and fabrication, is promising to greatly advance the quest for miniaturized and highly performing neural interfaces that can be worn on the scalp or implanted in the brain for a considerable duration of time. [2, 3] One of the main distinctions among neural interfaces is whether they are used as intracranial implants (invasive) or as non-invasive, wearable EEG types of neural sensors. Obviously, the requirements and areas of application of such sensor types are quite distinct. [4]

Neural implants are expected to benefit clinical applications, including deep brain stimulation and mind-controlled prosthetics. The implants need complicated surgery and have very stringent biocompatibility requirements. They have access to deeper brain structures and can access neuronal activity from a much more spatially confined area than EEG sensors. Early electrodes used in invasive or implanted sensors typically contained bulky metal-based electrodes, with severe issues of corrosion and tissue damage over prolonged operation. [5-8]

On the other hand, external neural interfaces of the EEG type are associated to a much lower risk for the user and can be used to non-invasively monitor brain states (including cognitive stress load and sleep patterns) and brain health, opening the possibility, for example to diagnose epilepsy, as well as potentially screening for and achieving an early diagnose of some of the neurodegenerative diseases. [9-12] In addition, non-invasive neural interfaces open the path towards all non-clinical hands-free control of autonomous external devices by harnessing the brain signals, including robotics, bionic prosthetics, neurogaming, consumer electronics, as well as autonomous vehicles. [13-15] The external devices can be controlled by the interpretation of human intention via detecting the cortical electrical activity, eye movement, and muscle movement through electroencephalogram (EEG), Electrooculography (EOG), and Electromyography (EMG), respectively, which all rely on non-invasive sensors. [6, 7, 13] The foundation concept of interconnecting external devices directly with brain signals was demonstrated by Hans Berger in 1929 by developing the first-generation EEG device using two channels with metallic needle electrodes to enable the non-invasive recording of neuro-electrical brain signals. [16] The first scientific study on volitional control of human brain oscillation was reported by Kamiya et al. in 1969, where the change of “alpha waves” (neural oscillations in the frequency range of 8-13 Hz) on continuous sensory feedback using EEG

channels at the C_4-O_2, C_z-A_2 positions had been demonstrated. [17] Since then, with the development of modern computer technology, numerous applications related to monitoring brain activities for healthcare and transferring brain signals to external electronics and computing devices for remote device controlling have been investigated. [18-23] Along with the medical applications of brain signal monitoring and recordings such as computer tomography (CT) scan, magnetic resonance imaging (MRI), and intracranial electroencephalography (iEEG) through implanted sensors, recently detecting the brain signal in a non-invasive approach to communicate with electronics devices have gained a lot of interest. [19-23] To adequately monitor and record EEG signals in non-invasive ways, wearable electrodes that are highly conductive, biocompatible, robust, with low and stable on-skin impedance and high signal-to-noise ratio (SNR) are necessary.

Conventional non-invasive EEG sensors are based on wet Ag/AgCl electrodes. Despite providing low contact impedance, wet electrodes have several limitations, including tedious and time-consuming preparation, skin irritation, hair fouling, loose control upon motion, and are unsuitable for long-term operation, particularly outside of clinical settings. [5-7] Hence, there is strong interest to obtain "dry" sensors that can perform as well as wet EEG sensors. Considering the need for continuous and prolonged operation, comfort, wearability, reusability, and robustness, sensors based on dry electrodes are generally preferred as advanced human-robot interfaces for applications that do not involve severe disabilities. [24-26] The development of hydrogel-based non-invasive electrodes reduced the amount of necessary gel/paste; however, the sensors retain some of the limitations of the wet sensors. [27] Some of the currently available dry EEG sensors are based on metal pins for contact on hairy areas, or on foam sensors covered by a highly conductive metal mesh. [7, 21] None of these solutions offer sufficient performance and therefore are one of the elements holding back the development of efficient brain-machine interface technologies. [5, 7, 28, 29]

The recent advances in the knowledge and technology around the use of 2D nanomaterials and their unprecedented functionalities in energy, catalysis, sensors, and electronics have warranted the investigation of their benefits as sensor materials for neural interfaces. [30-35] Among the promises that some of the 2D materials hold are extreme miniaturization, high surface contact area, exceptional biocompatibility, functionalization capabilities, and electrical conduction.

This review focuses on the latest advancements in invasive and non-invasive sensors for neural interfaces using two-dimensional (2D) materials - primarily graphene, [30] MXenes as group of

2D early transition metal carbides, nitride, or carbonitrides, [31] and transitional metal dichalcogenides (TMDs). [35] The schematic in Figure 1 shows the types of neural interfaces where electrodes based on 2D materials can be employed to record biopotentials in both invasive and non-invasive ways. We will first describe the few available examples of electrodes made of 2D nanomaterials in invasive neural interfaces and their future direction. We will then focus on recent advances in non-invasive thin-film sensors based on 2D materials for healthcare and brain-computer interfaces. Lastly, we will conclude this review with a section about the ongoing challenges for non-invasive interfaces.

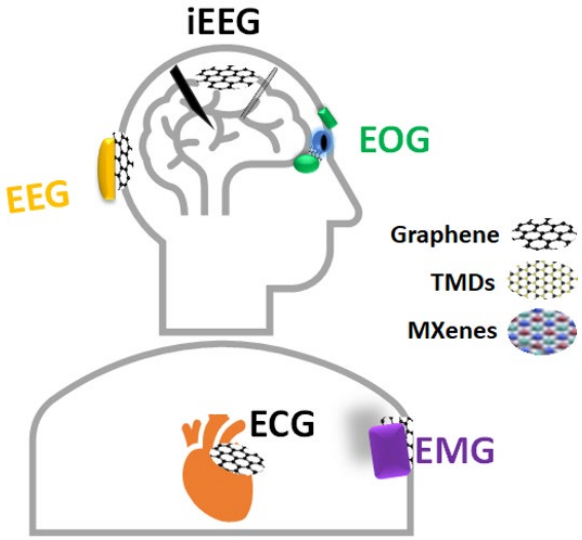

Figure 1: Schematic indicating different types of implanted and wearable neural interfaces that could benefit from the use of 2D materials electrodes (graphene, MXenes, TMDs).

2. INVASIVE NEURAL INTERFACES

Thin-film electrodes made of highly conductive and biocompatible material which can be precisely micropatterned constitute a preferred approach to intracranial electroencephalography (iEEG) with implantable bioelectronics. [22, 34, 36] Both silicon and polymer-based electronics using a conductive metal layer of gold, platinum, titanium, or carbon as neural electrodes, either as an array or as filament, have been investigated as implantable approaches. They have demonstrated passive sensing as well as stimulation capabilities when applied either onto the surface or deeper in the heart and the brain of lab animals. [37-45]

Advanced electrodes for iEEG and neurostimulation can have a variety of shapes and approaches (Figure 1), but for simplicity are mainly classified into three types: flexible filament

or wire deep probes, multielectrode microarray probes, and planar microelectrodes. [22, 39] The planar microelectrodes are typically placed on the surface of the brain cortex to record electrocorticography (ECoG), which offers a superior spatial resolution to non-invasive EEG. [40] A recent example of commercial application of ECoG is demonstrated by "Neuralink" where 96 fibrous electrodes of around 4 to 6 μm in width are made of three conductive layers of gold, iridium oxide and the conductive polymer PEDOT:PSS (poly-ethylenedioxythiophene doped with polystyrene sulfonate) to lower the impedance (37 ± 5 kΩ at 1kHz) and enhance the charge-carrying capacity.[38]

A critical challenge for the implanted interfaces is the ability to ensure a sufficient level of biocompatibility of the used materials and overall system, able to stymie adverse effects of long-term implantation on both the biological and the sensing systems. Amongst the potential issues arising are a corrosive interaction of biofluid with the active metallic electronic components, and electrical leakage current leading to damage to the surrounding biological tissues.[22] The coating of thin-film membrane electrodes for iEEG with biocompatible polymers (such as polyimide, polyurathane, polydimethyl siloxane, and parylene C) have been shown to improve performance and long-term stability, thanks to a minimal contact of the biofluid with the metals (platinum, gold, titanium) electrodes. [38-41] Note that in the context of biocompatibility, the availability of miniaturised electrodes using nanomaterials is expected to offer at least a partial relief thanks to their nanometric sizes. [42]

2.1 Graphene-based Invasive Interfaces: Nanostructured two-dimensional materials, especially graphene, have been investigated to alleviate persistent challenges around achieving high conductivity with very thin layers/probes, high signal-to-noise ratio, biocompatibility, reducing corrosion, and biological fluid interaction. [43-49] The high electrical conductivity, surface functionality, and unique two-dimensional flat structure of graphene makes it a promising choice for advanced neural electrodes. [45] Incorporating graphene in advanced electrodes for neural sensing could enhance biocompatibility without the need for polymer protective coatings, and also improve signal-to-noise ratio and increase long-term stability.[50-56] The availability of different forms of graphene such as single layer CVD graphene, few-layer exfoliated graphene, epitaxial graphene, chemically processed graphene platelets, mechanically exfoliated graphene nanoplatelets, graphene oxides, and hetero-atom doped graphene provides a broad versatility for their choice as electrode material for iEEG . [57-62]

2.1.1 Flexible Filament Probe: A graphene-based binder-free microfiber has been employed for neural recording to replace filament-shaped metallic neural electrodes. [50-52] The binder-free high mechanical strength fibre formation by manipulating the liquid crystalline properties of ultra-large flakes of graphene oxide showed improved performances both on specific contact impedance (3.9 ± 0.4 MΩ μm^2 at 1kHz) and charge storage capacity (361 ± 45 mC cm^{-2}) compared to the conventional filament-shaped metallic microelectrodes for neural interfaces. [50] The graphene fiber was coated with a platinum layer as the current collector and parylene C coating as an insulator. The schematic of the fabrication of graphene fiber is presented in Figure 2a. [50]

2.1.2 Planar Microelectrodes: Graphene based flexible flat micro-electrodes directly grown on polyimide surface using laser pyrolysis has been employed for electrocorticography. [43] In parallel, planar microelectrodes incorporating graphene field-effect transistors (FETs) have also been developed for ECoG, assisting with local amplification and transduction of the biological signals. [44, 53-55] In this approach, the graphene channel was placed in contact with an electrolyte gate that referred as graphene solution gate field effect transistor (g-SGFET). [53] It was fabricated by transferring CVD-grown graphene on a Si/SiO_2 wafer patterned by photolithography and etched to form planar microelectrode arrays of graphene channels. Its operation had been demonstrated utilizing brain tissue as gate electrolyte (Figure 2b). [53] These advanced electrodes opened up the possibility of multiplexing the multiple signals transmitted through the channel. The graphene FET microelectrode array showed continuous mapping for ~24 h of wide frequency band epicortical brain activity by evaluating infra-slow (<0.5 Hz) brain activity (ISA) patterns during distinct brain states. [54, 55]

The optically transparency of graphene provides the opportunity to develop transparent graphene microelectrodes to perform simultaneous optical imaging and electrophysiological recording with ECoG. [49, 56] Microelectrodes array for neural imaging and optogenetic have been fabricated by patterning graphene using a silicon wafer as a sacrificial template, and coating the outer layer with parylene C as insulator layer (Figure 2c (i)). [56] The reported micro-electrocorticography electrode exhibited an impedance of 243.5 ± 5.9 kΩ at 1 kHz in saline solution. The fabricated transparent electrode implanted on the cortex of a mouse, recorded the neural signal efficiently from the generation of stimulation by the blue light stimulus (Figure 2c (ii)). [56] Transparent micropatterned graphene electrodes have been also reported for deep two-photon imaging in optogenetic applications. [57, 58]

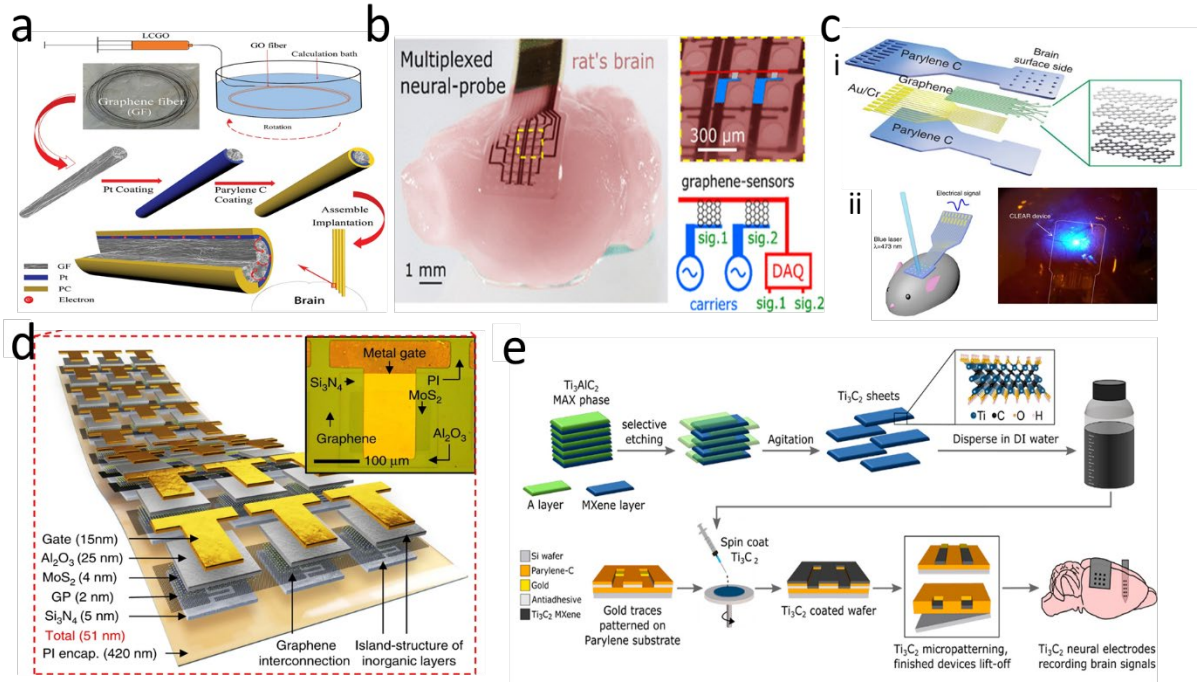

Figure 2. a) Schematic of the process of graphene fibre-Pt microelectrode from graphene oxide fibre. Reproduced with permission from ref. 50. Copyright 2019 Wiley. b) Graphene-based micro-array thin-film invasive sensor to collect signal from rat's brain. Reproduced from ref. 53. Copyright 2020 American Chemical Society. c) Schematic of optically transparent graphene thin-film sensor fabrication. i) showing the layered structures, ii) schematic drawing of the device implanted on the cerebral cortex of a mouse and the detection of the signal by blue light stimuli to the neural cells. Reproduced with permission from ref. 56. Copyright 2014 Springer Nature. d) Schematic of the design of graphene-MoS_2 hetero-structured image sensor array device. Inset shows the microscopic image of a single phototransistor. Reproduced with permission from ref. 65. Copyright 2017 Springer Nature. e) Schematics of synthesis and atomic structure, fabrication and application of Ti_3C_2 arrays for recording brain activity in the rat brain. Reproduced from ref. 67. Copyright 2018 American Chemical Society.

2.1.3 Multielectrode Array Deep Probe: A flexible graphene microelectrode array-based deep probe has been reported to record full-bandwidth electrophysiology of seizures and epileptiform activity. [59] Here the depth probe is consisted of a linear array of graphene microtransistors, to concurrently record high-frequency neuronal activity in awake rodents over 10 weeks. [59]

2.2 MXenes for Planar Microelectrodes: Next to graphene, also MXenes have gained attention as electrode material for neural interfaces, thanks to their high electrical conductivity

and capacitive properties. [66, 67, 68] In MXenes, n + 1 (n = 1–3) layers of early transition metals (M) are interleaved with n layers of carbon or nitrogen (X), with a general formula of $M_{n+1}X_nT_x$. The T_x in the formula represents the surface terminations, such as O, OH, F, and/or Cl, which are bonded to the outer M layers. [68] Detailed studies on the biocompatibility and cytotoxicity of MXenes are still ongoing. [69] The cytotoxicity of MXene is dependent on the functional groups (-F, –OH, and –O), flake size (1–100 nm), oxidative state, and layer numbers. [69-72] Among the limited number of studies, it has been observed that the titanium carbide (Ti_3C_2) based MXenes with low concentration (12.5 µg/mL) did not show any observable adverse effect on the neural cell, especially in cellular uptake and cell membrane integrity. [70]

As an example, the Ti_3C_2-MXene based microelectrode array fabricated *via* spin coating of an aqueous dispersion of Ti_3C_2 on a gold patterned parylene C substrate performed as micro-ECoG and intracortical electrodes for *in vivo* neural recording without observing any cytotoxicity (Figure 2e). [67] This ECoG electrode with an overall thickness of ~10 µm and a diameter of 25 µm indicated a 4-fold lower impedance compared to gold electrodes (219 ± 60 kΩ for Ti_3C_2 and 865 ± 125 kΩ for gold at 1 kHz) as well as higher signal to noise ratio.

2.3 Challenges and Future Directions: Overall, while graphene is reaching some level of maturity, the investigation of additional 2D materials for invasive neural sensors is still at a very early stage. In addition to graphene and MXenes, we suggest that the unique combination of atomic-scale thickness, direct bandgap, strong spin–orbit coupling, electronic and mechanical properties of TMDs, makes them attractive for investigation in neural interfaces. [35, 73-79] A graphene-MoS_2 phototransistor was demonstrated as image-sensor device (Figure 2d) for optogenetic applications. [65] A recent report also indicated the use of CVD-grown MoS_2 to develop a bioabsorbable sensor for intracranial monitoring of pressure, temperature, strain, and motion on a rat for brain injury monitoring. [79]

Table 1. Overview of some prominent examples of invasive neural sensors based on 2D materials and related characteristics.

Invasive neural interfaces	Application	Contact impedance	SNR	Stability tests	Ref
Porous graphene array by laser pyrolysis *(Planar electrodes for ECoG)*	Neural recording	5±3 kΩ at 1 kHz	N/A	1 x 10^6 cycles	43
Doped single layered graphene *(Planar electrodes for ECoG)*	Neural recording	541 kΩ at 1kHz	40.8	6 months in phosphate-buffered saline	49
CVD graphene based transparent micro-array *(Planar electrodes for ECoG)*	Neural imaging & optogenetic	243.5±6 kΩ at 1 kHz	N/A	70 days after implantation	56
Ti3C2-MXene based microelectrode array *(Planar electrodes for EcoG)*	Neural recording	219±60 kΩ at 1 kHz	40	7 days in cell culture	67
Ti3C2-Mxene electrode array *(Planar electrodes for EcoG)*	Neural recording	54.6 ± 28.4 kΩ at 1 kHz	N/A	N/A	68
Liquid crystal GO fiber coated with Parylene C *(Filament deep probe)*	Neural recording	50±10 kΩ at 1 kHz	N/A	14 days in phosphate-buffered saline	50
Graphene multielectrode array *(Microtransistor -based deep probe)*	Neural recording	N/A	N/A	> 10 weeks implanted	59

Table 1 shows an overview of invasive neural interfaces using 2D materials and their main characteristics. Note that direct comparisons are very difficult because of the varied nature of the sensing approaches. Overall, more detailed and long-term research on their reliability, including the various aspects of biocompatibility, cytotoxicity, electrical and contact stability, mechanical compatibility (flexibility and modulus matching aspects) [23, 78. 79] will all be necessary to assess the suitability of 2D materials for invasive neural interfaces.

3. NON-INVASIVE NEURAL INTEFACES

In the following sections, we will describe the advancement of 2D materials for fabricating thin-film electrodes for non-invasive neural interfaces: their material selection, fabrication, and final performance in a biosensor. The following sections are organized on the basis of the different fabrication substrates and platforms, all leading to distinct performances and opportunities. Once again, the investigation of graphene has produced to-date substantially more literature as compared to other 2D materials. One aspect to note is that in most cases, the use of reduced graphene oxide, or a graphene with tailored functionalisation is generally preferred to the use of low-defect graphene, due to its high hydrophobicity in its pristine state. [80]

3.1 Graphene on Polymer: Polydimethylsiloxane (PDMS) is a common substrate polymer for developing thin-film-based non-invasive wearable sensors to detect biopotentials. [81] Typical PDMS-based flexible sensors are fabricated by either coating, spraying, electrostatic spinning, or sputtering of the conductive metal layer (e.g., Silver, gold, platinum, titanium) on the surface of the skin-mounting side. [81] Micro-patterned reduced graphene oxide on PDMS was used to develop a flexible on-skin neural sensor that can measure electromyography (EMG), electrooculogram (EOG), and electroencephalogram (EEG) signals with high fidelity with low skin-electrode contact impedance. [82] This sensor, aimed at controlling bionic hands, was demonstrated to recognize five typical hand gestures (spherical grasp, cylindrical grasp, tripodal grasp, lateral grasp and precision grasp) with more than 75% accuracy. The sensor pattern was prepared using a mechanically cut adhesive tape pasted on a silicon substrate and chromium and copper sputtering deposition. The silicon with the metal pattern was then kept in GO solution at elevated temperature to obtain the rGO pattern and transferred onto a PDMS substrate. This flexible electrophysiological sensor can form on-skin conformal contact with stable connection and low contact impedance of ~ 500 kΩ at 50 Hz by using thin Au/Cr coated PET straps to bond the rGO and the external conductive wires. [82] In addition to PDMS, PET and PI-based substrates have also been used to fabricate graphene thin-film sensors. [83, 84] The laser-reduced GO on PET substrate demonstrated extended stability in a harsh environment over 100 h as an ECG electrode due to the formation of chemical bonding between the rGO and PET substrate by laser treatment as well as the conductive connection formed by gluing a copper wire to the rGO by silver paste. [83] The one-step fabrication of this bioelectrode was conducted by drop-casting GO solution on the top and bottom surface of the PET substrate, covering the whole top surface with GO. A controlled laser performed the GO reduction at a

wavelength of 405 nm. The arbitrary-shaped lased-reduced GO thin-film sensor showed on-skin impedance of ~60 kΩ at 10 Hz for ECG monitoring. [83] The open mesh-shaped graphene/PI sensor fabricated by aerosol jet printing of graphene solution on a sacrificial template of PMMA showed reduced on-skin contact impedance of ~200 ± 10 kΩ at 100 Hz as an integrated soft, wireless bioelectronic system for EEG based sleep monitoring. [84] To avoid the complexity of the graphene transfer, a direct graphene coating on polymer substrate process has been reported to fabricate rGO/Nylon dry epidermal sensor. [85] In this process, the GO hydrogel is synthesized by hydrothermal reaction passed through a nylon membrane by vacuum filtration to form the graphene layer on nylon and heated to reduce the graphene oxide. This flexible, biocompatible, highly conductive (~40 Ω/sq) sensor identified the alpha rhythm with the blinking of eyes at the alpha band (8-14 Hz) in a similar way as commercial Ag/AgCl gel sensors. A low on-skin impedance of ~15 kΩ at 100 Hz was reported, and was implemented as ECG, EMG, and human-motion monitoring devices. [85]

Recently, ultra-thin (~100 to 500 nm) polymer-based skin-mimicking sensors, often labelled as electronic-skin (e-skin), or wearable cloth sensors fabricated with graphene-coated yarn (e-textrode), have gained ample interest. [86, 87] The advancement of these graphene/polymer-based ultra-thin film sensors is discussed below.

3.1.1 Graphene E-Skin: Ultra-thin, skin-inspired soft epidermal electronics, or e-skin, has been developed for health monitoring, prosthetics, and soft robotics. [88, 89] One example is the graphene integrated with an ultra-thin open-mesh structured e-tattoo sensor that monitors simultaneously biopotentials, skin temperature and hydration. [90] The fabrication steps of the tattoo sensor followed the typical “wet transfer” process like that of graphene/ polymer thin-film sensors except, for an additional step of “dry patterning’ directly on tattoo paper. This graphene tattoo sensors showed applicability for human-robot interfaces by capturing the EOG signals from eyeball movements to command a drone to fly according to the eyeball direction. [91, 92] Like e-tattoo sensors, e-skin sensor fabricated by laser scribed graphene on a polyurethane nanomesh can be used as flexible skin-attached electrodes for EEG monitoring (Figure 3a). [93] The dry e-skin sensor showed lower contact impedance for frequencies below 1000 Hz and higher signal-to-noise ratio compared to commercial gel electrodes (14.1 dB for e-skin, versus 10.7 dB for the gel electrode). [93]

The CVD graphene-coated conductive polymers (PEDOT:PSS)-based transparent ultra-conformal on-skin sensor showed with low sheet resistance (~24 Ω/sq) and enhanced

performance as human-robot interfaces such as facial expression-controlled robots, brain activity in motion, and long-time EOG and EEG signal monitoring (Figure 3b). [94] This work has overcome the fabrication limitation of conductivity and wettability of PEDOT: PSS on the top of transferred CVD graphene by adding surfactants (sodium dodecyl sulfate) and ionic compound (bis(trifluoromethane) sulfonimide lithium salts) during spin coating. [94]

3.1.2 Graphene E-Textrodes: Graphene-coated textile yarns (e-textile) have been investigated as sensing electrodes for long-term repeated on-skin signal monitoring, including EOG, EMG, and EEG. [95-99] The GO solution or rGO dispersion are the best choice of materials for dip-coating the yarns (such as nylon, cotton, polyester) to form graphene-coated fibres. [95, 97] The successful acquisition of EOG signal by detecting eye movement for human-computer interface using graphene textile electrodes was first reported by Golpavar et al. [95] In this work, the conductive textrodes were fabricated by dipping the fibers on GO solution followed by reduction *via* hydrazine. The sheet resistance of the prepared electrodes (~3 x 3 cm) was found ~ 20 kΩ /sq. This graphene-coated textiles have also been employed for EEG activities by detecting alpha rhythms from the forehead with an excellent correlation of ~91% compared to the commercial dry sensors. [97] The one-step dying process with GO and further layer by layer dip-coating process with conductive polymer (PEDOT:PSS) on nylon-lycra fabrics showed improved conductivity (~50 kΩ/sq) for detecting ECG signals (shown in Figure 3c). [100] This e-textrode showed good stability in repeated uses for up to 20~30 washing and 120~130 bending cycles. [100] The further modification of this work by introducing post-treatment with organic solvents, reduced the sheet resistance down to 130 ± 0.5 Ω, that is highly suitable for detecting the pulse rate response. [101] The high-speed yarn dying with graphene ink has been proven better approach for fabricating full textile cloths compared to dip coating of the knitted fabrics for developing smart textiles. [96] The recent advancement of electrospinning, a process to produce fine filaments from drawing a polymer solution using a strong electrical field, showed as an alternative approach to fabricate soft wearable electronics as on-skin sensors. [102] The advantage of the electrospinning-based filaments is the ability to deposit or embedded the conducting materials like graphene onto elastomeric substrates to make the electrodes. [102, 103] An example is the durable, non-disposable transparent electrode for detecting key biometric signals such as ECG, EMG, and EEG (Figure 3d). [104] This high conductive (~150 Ω/sq) and transparent (83% transmittance) e-textrode was fabricated by electrostatically spinning the polymer (Polystyrene-block-poly(ethylene-ran-butylene)-block-polystyrene (SEBS)) on CVD grown graphene on copper foil and then annealed at 600 °C for half an hour. This on-skin

sensor demonstrated robust performance under mechanical stress with unique aqueous washability and repeatability (~10 repeats) with high SNR (~30 dB) for detecting EMG. [104]

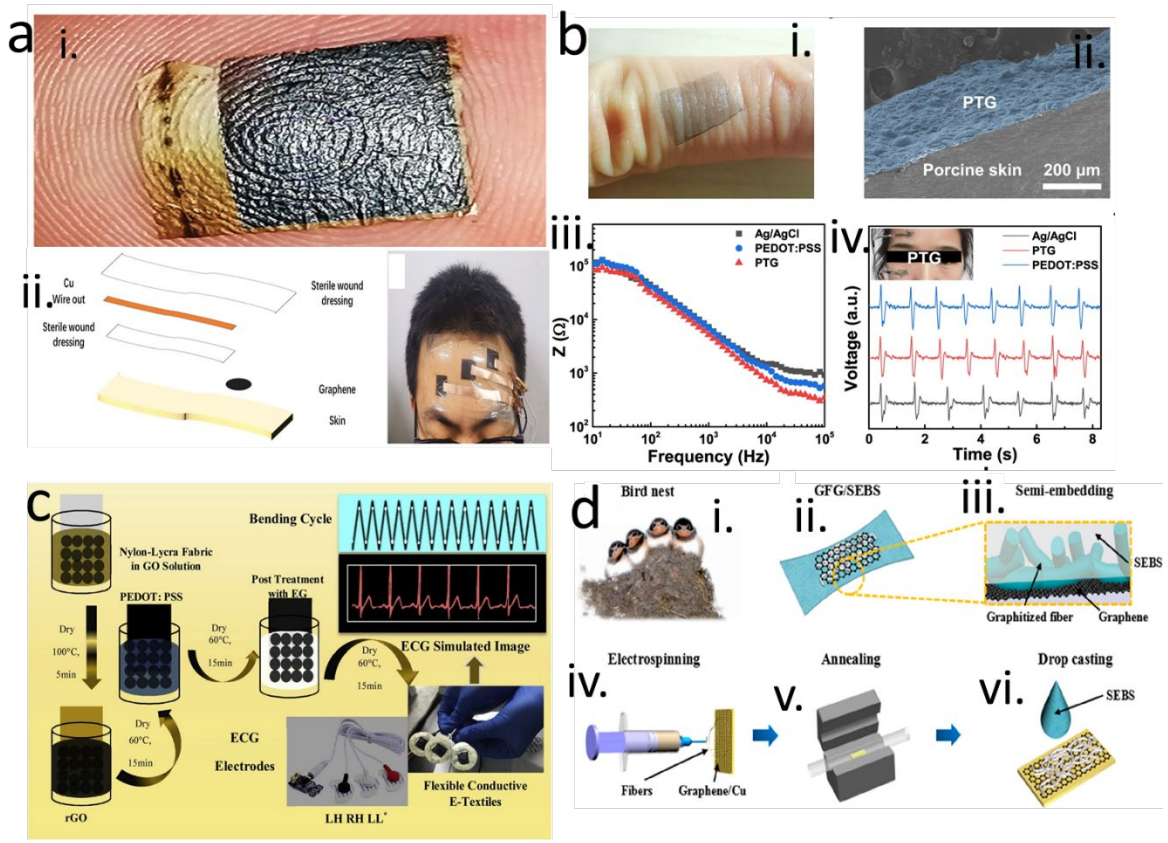

Figure 3. a) i) Photographic image of the LSG/PU nanomesh on a finger showing the fingerprint morphology (the yellow film is GO/PU while the black film is LSG/PU, respectively), ii) Schematic diagram of the EEG e-skin fabrication and the EEG e-skin attached to the forehead of the tester. Reproduced with permission from ref. 93. Copyright 2022 Wiley. b) i. Photograph of PEDOT:PSS transferred CVD graphene (PTG) film conformed on skin. ii. SEM image of PTG (top) on porcine skin (bottom). iii. The electrochemical impedance spectroscopy (EIS) of PTG (red), pure PEDOT:PSS (blue) and Ag/AgCl (black) electrodes. iv. EOG measured by PTG (red), pure PEDOT:PSS (blue) and Ag/AgCl (black) electrodes, showing peaks and valleys corresponding to the eyelid movement. Reproduced with permission from ref. 94. Copyright 2021 Springer Nature. c) Schematic diagram of rGO-PEDOT:PSS coated nylon-lycra fabric based e-textrode for ECG analysis. Reproduced with permission from ref. 100. Copyright 2020 Elsevier. d) Schematics of fabrication of semi-embedded graphitized electrospun fiber/monolayer graphene (GFG) as non-disposable graphene-based skin-electrodes. (i) Schematic of a bird's nest, which was mechanically reinforced by tightly connected polysaccharide. (ii, iii) Schematic of GFG film semi-embedded

in SEBS elastomer with a cross-sectional view (panel (iii)). (iv-vi) Schematic fabrication process of GFG. In panel (iv), the polymer fibers were electrostatically spun on the surface of graphene grown on Cu foil by CVD. In panel (v), the fibres/graphene/Cu foil were annealed under an atmosphere of argon. In panel (vi), SEBS solution was drop cast on their surface and semi-embedded into the entire structure of fibres/graphene/Cu foil. After the copper was etched away, semi-embedded GFG film was formed as illustrated in panels (ii) and (iii). Reproduced from ref. 104. Copyright 2021 American Chemical Society.

3.2 Graphene on Silicon Carbide: Silicon Carbide (SiC) is a suitable substrate material for biological interfaces thanks to its inertness, corrosion resistance against biological fluids, lightweight, bio and hemo-compatibility. [105-107] Recently, we have demonstrated epitaxial graphene grown on a highly doped conductive silicon/silicon carbide wafer (resistivity ~10-20 Ω.cm) as a robust, long-term stable, non-invasive, on-skin neural sensor that outperformed commercial dry sensors. [80]

The epitaxially grown 3C-SiC on silicon can be graphitized selectively at the wafer scale utilizing common silicon processing methods such as, photolithography, etching, spin-coating, sputtering, thin-film formation and integrated circuitry. [108-117] The graphene is grown epitaxially on a 3C-SiC on silicon pseudo-substrate using a catalytic alloy of nickel and copper to grow epitaxial graphene on silicon at a relatively low temperature (~1100°C). [110, 111] Uniform, highly conductive graphene [114] can be obtained selectively at the wafer-scale, [112] with sufficient adhesion to its substrate. [117] The use of a highly-doped silicon substrate underneath the SiC film leads to strong carrier inversion at the SiC/Si interface, which becomes conductive. [119] This phenomenon allows to create an effective electrical conduction from the epitaxial graphene electrode in contact with the skin on the one side, through to the silicon backside, which can subsequently be further connected to the socket of a helmet or band system (Figure 4a). This highly robust on-skin sensor showed successful detection of alpha rhythm with the blinking of the eyes and a forehead contact impedance of 68 ± 4 kΩ at 10 Hz. A key aspect in the achievement of a low and stable contact impedance with the skin with this sensor is the formation of a thin boundary layer of water on the graphene surface upon contact with the skin, facilitated by the small grain size (~ 100 nm) of this epitaxial graphene. The surface conditioning phenomenon allows for a substantial decrease of the contact impedance of the graphene sensor with the skin within the first few minutes of contact, and shows high

robustness in saline solution. This sensor type, although rigid, possesses amongst the best reliability data for long-term, extended and repeated usage. It showed no degradation in performance after immersion in 3M sodium chloride solution for 120 days. [80]

3.3 Graphene on Silicon and Silicone elastomer: An alternative approach using graphene on silicon is given by graphene grown around silicon nanowires by plasma-enhanced CVD and is referred to as 3D fuzzy graphene. [120] This three-step process was initiated by synthesizing silicon nanowires first using gold nanoparticles as a catalyst in the vapor-liquid-solid (VLS) process and then forming an interconnected mesh of nanowires; lastly, graphene is grown out of the plane surface through PECVD process. [120] This 3D fuzzy graphene microelectrode showed good electrical conductivity with sub-cellular recording capability of neural signals. [121, 122]

Finally, a laser-induced transferred graphene on highly porous sugar-templated silicone elastomer substrate has been reported as a flexible, breathable, and stretchable on-skin sensor. [123] The micro-patterned of the porous graphene was first synthesized by converting PI *via* the photothermal process. The patterned graphene was then transferred onto semi-cured elastomer/sugar composite substrates, and lastly, the on-skin sensor was fabricated by curing at room temperature, followed by removing the sugar *via* dissolving in water (Figure 4b). This simple fabricated patterned sensor without photolithography and etching showed efficient performance in detecting EEG, ECG, and EMG signals, including alpha rhythm at 10 Hz for EEG with a low skin-contact impedance of ~17 kΩ at 100 Hz. It also shows a high signal-to-noise ratio of ~24.1 dB for ECG signals. [123]

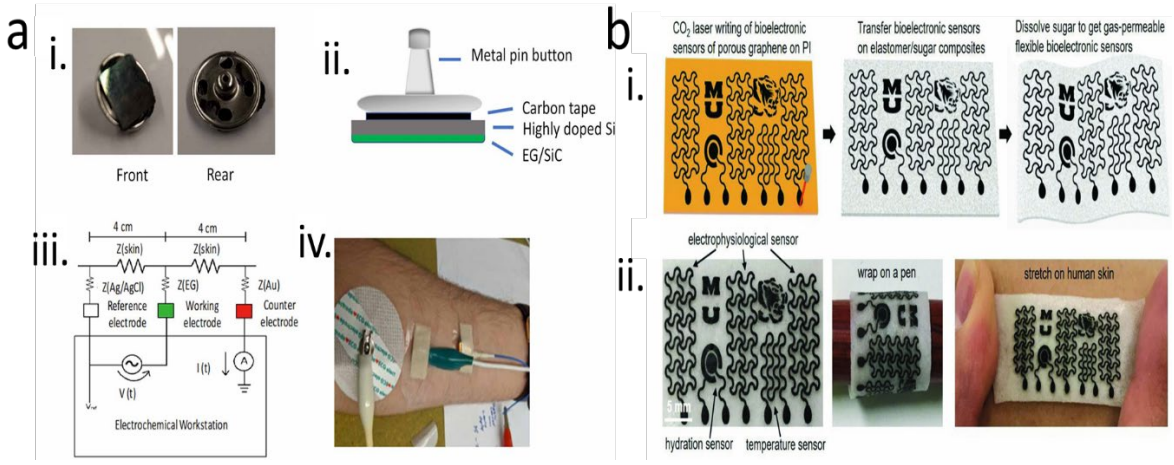

Figure 4. a) i) The epitaxial graphene (EG) sensors mounted on a metal pin button with carbon tape; ii) schematic showing the approach for the EG sensor. iii) Equivalent circuit diagram of

the on-skin EIS measurements, and iv) the on-skin EIS setup on the forearm. Reproduced with permission from ref. 80. Copyright 2021 IOP Science. b) i) Schematic of the fabrication of on-skin bioelectronic sensing systems using porous graphene. ii) Optical images of the as-made on-skin bioelectronic sensing systems. Reproduced with permission from ref. 123. Copyright 2018 Wiley.

3.4 2D Materials Beyond Graphene: Alternate two-dimensional materials beyond graphene have gained attention for skin-mounted electronics and non-invasive thin-film interfaces. [88] MXenes, in particular the Ti_3C_2-MXene, has been used as electrode material for fabricating neural sensors for its high conductivity, biocompatibility, micro-fabrication, and aqueous processability. [67] A $Ti_3C_2T_x$-MXene high-density microelectrode-array thin-film sensor has been developed for non-invasive EMG, EEG, and EOG signal monitoring and detection. [124, 125] The 16 micro-electrode channels contained thin-film sensor (thickness ~ 8 μm) was fabricated through integrating spray-casting process to precisely pattern $Ti_3C_2T_x$ along with photolithography, e-beam deposition, and lift-off process on the parylene C substrates. [125] These micro-fabricated sensors showed excellent on-skin impedance of ~ 29.78 ± 8.18 kΩ.cm^2 at 1 kHz with high SNR of 39.23 ± 16.25 dB for identifying a distinct region of muscle activation by high-resolution mapping in the thenar eminence muscle group. [125] Further improvement in the fabrication process had been carried out by introducing laser patterning on an MXene ink-infused nonwoven cellulose-polyester substrate to make 3D MXtrode arrays. [68] The "mini-pillars" of MXene-infused cellulose were attached to the laser-patterned substrate and encapsulated by PDMS with manual trimming to expose the conductive side. These dry 3D MXtrodes arranged in a ring successfully acquired high-resolution scalp EEG for alpha rhythm in the closed eyes state with significantly higher amplitude than in the open eyes state by placing over the parietal region over short hair (~5 mm) with a low skin impedance of 2.8 ± 0.9 kΩ at 1 kHz (Figure 5a). This new class of sensors also showed efficient signal recording from EMG, EOG, Cortical neural recording, and micro-stimulation that established the MXtrode as an alternative electrode material for the brain-machine interface. [68]

Along with the MXenes, two-dimensional TMDs have been investigated for non-invasive neural sensors. [118, 127] The recent work on platinum-based two-dimensional TMDs (platinum diselenide ($PtSe_2$) and platinum ditelluride ($PtTe_2$)) as reusable electronic tattoo sensors for EEG, EMG, EOG, ECG, and thermal sensing has demonstrated better performance compared

to the previously reported graphene-based tattoo sensors. [128] Here the $PtSe_2$ and $PtTe_2$ based thin film micro-patterned sensors synthesized by growing through a thermal-assisted conversion (TAC)-based low temperature (400°C) CVD process on Kapton and then cut into micro-patterned shaped using a cutter-plotter tool (Figure 5b). The $PtTe_2$ tattoo sensor offered the lowest on-skin impedance of 4.94 ± 1.61 kΩ at 10 kHz along with a high signal-to-noise ratio (SNR) of 84 ± 6 dB for ECG recording. This sensor has also been employed to detect EMG, EOG, and EEG. The detectability of alpha waves has been demonstrated by placing the two electrodes on the forehead in Fp1 and Fp2 regions, picking up the spectrogram patterns for closed eyes. [128] In parallel with Pt-TMDs, MoS_2-based highly stretchable free-standing van der Waals (VDW) thin-film with breathability for monitoring electrophysiological signals has been reported very recently. [129] This novel approach of free-standing thin film (thickness ~10 nm) fabrication with bond-free VDW interfaces of the two-dimensional nanosheets enabled sliding and rotating degrees of freedom to deliver extraordinary mechanical flexibility as well as create a new type of sensing platform by utilizing the intrinsic properties of interacted assemble of two-dimensional materials mimicking biological assemblies. [129] The overall performance of the reported non-invasive 2D material-based thin-film neural sensors is described in below Table 2.

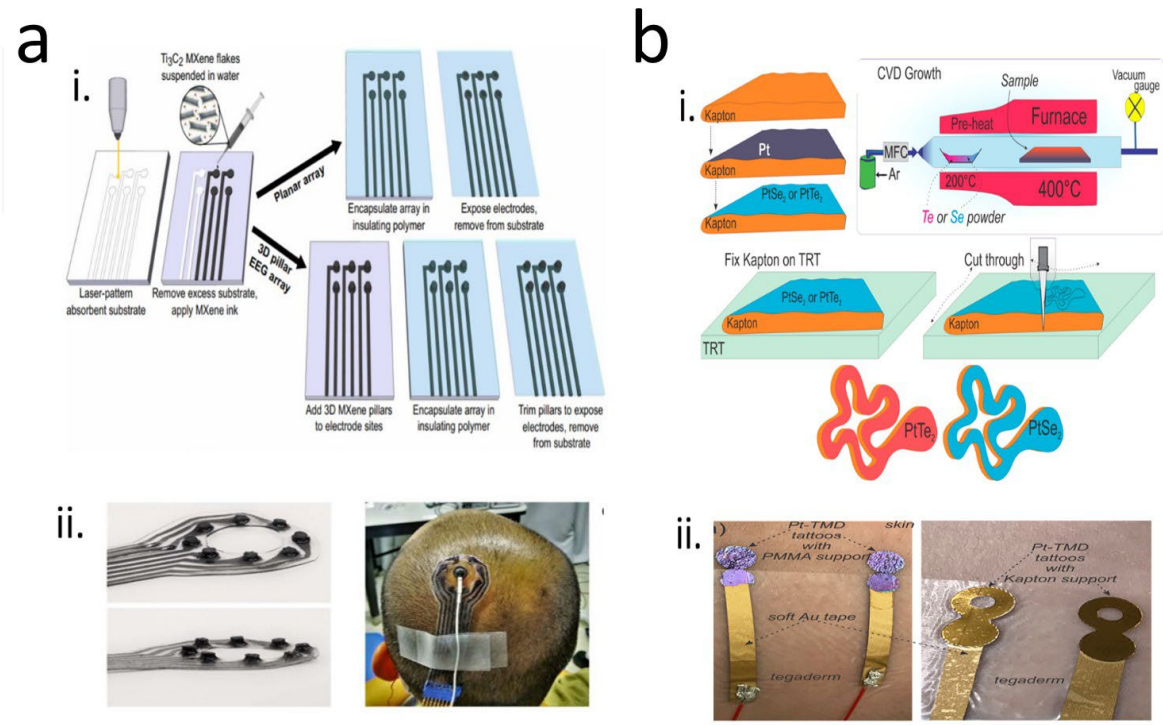

Figure 5. a) i) Schematic of the fabrication process for laser-patterned MXene electrode arrays. ii) Photographs of 3D designed MXtrode EEG electrode array with Ag/AgCl electrode placed on the head of a human subject. Reproduced with permission from ref. 68. Copyright 2021 AAAS. b) i) Schematic of Pt-TMD tattoo design and fabrication process. ii) Photographs of Pt-TMD tattoos, with PMMA (left) and Kapton (right) polymeric support with electrical contacts. Reproduced from ref. 128. Copyright 2021 American Chemical Society.

4. CHALLENGES AND FUTURE DIRECTIONS FOR NON-INVASIVE INTERFACES

4.1. Electrical Performance: The majority of the current neural interfaces are based on the electrochemical sensing of summated biopotentials from a very large population of neurons from the brain cortex. Low contact impedance and high signal to noise ratio (the dimensionless ratio of signal power to noise power) are key requirements for the sensors in order to detect the μV amplitude signals of the cortex signals. Among the non-invasive on-skin sensors, Ag/AgCl wet sensors still demonstrate the lowest on-skin impedance of ~ 30 ± 5 kΩ at 100 Hz. [81, 130, 131] In general, achieving a similarly low on-skin impedance with dry sensors is still challenging. However, the discussed e-skin sensors composed of conductive polymer (PEDOT:PSS) and CVD graphene (on-skin impedance of ~ 35 kΩ at 100 Hz), [94] epitaxial graphene sensor (on-skin impedance of ~ 80 kΩ at 100 Hz), [80] and laser-induced porous graphene (on-skin impedance of ~17 kΩ at 100 Hz) [123] all demonstrate competitive values, reasonably close to that of wet sensors (Table 1). Further advances in the micro-fabrication and understanding the charge transfer process of 2D materials at the interface with the skin [80] may lead to dry sensors matching the impedance of the wet sensors.

Note that improvements in all aspects of electrical performance of non-invasive neural interfaces will need to come from the engineering of the whole system, in addition to improvements of the electrode materials.

There are various factors influencing the SNR of an EEG sensor, and they can be either extrinsic like the collection of unwanted neural responses from the surroundings of the targeted site, or intrinsic to the sensor system and its contact to the skin. The contact impedance of the electrode to the skin is only one of the factors determining the electrode SNR, which is also frequency-dependent. [132] There are various other sources of potential noise in the sensor system, including the chosen reference electrode type and site. When benchmarking SNR of a

sensor, it is hence important to compare using the same system. One has to be cautious when comparing directly SNR of different electrode material across different EEG systems.

Overall, Ag/AgCl wet sensors still tend to provide a more favourable signal to noise ratio. [128] However, the recent work on the $PtTe_2$ tattoo sensors showed higher signal to noise ratio (84 ± 6) in ECG measurement as compared to Ag/AgCl (61 ± 5). [128]

4.2 Comfort and Durability: Long-term health monitoring, controlling of prosthetics or other external robotic devices may require continuous operation and repeated use. The metal-free graphene on soft polymers-based e-skin and e-textrode demonstrated long-term operation for up to several days (table 1). In general, the reported tattoo-like e-skin sensors tend to be disposable and not suitable for re-use; [90] however, the discussed e-textrode sensor fabricated by graphitized electrospun fiber/monolayer graphene showed capability for washing and repeated use up to ~ ten times. [104] Another aspect that restricts the repeated use of the graphene sensors is generally the delamination of the graphene from the polymer substrate upon prolonged use. [85] The epitaxial graphene grown on silicon/silicon carbide showed excellent stability (> 120 days in 3M salt solution) and over repeated and long-term use thanks to the strong adhesion of the graphene with the underlying substrate. [80]

Soft electrodes in open, fractal mesh geometries may adapt better to the morphology of the auricle and the mastoid as reference electrodes, which is not possible with rigid electrodes. [133] The gold coated (500 µm thick) on PI based flexible substrate demonstrated attachment on the auricle and mastoid using van der Waals interactions as well as PVA-based water -soluble adhesive as polymer backing layer that allowed continuous monitoring for 24h. [133]

Table 2. Overview of some prominent examples of non-invasive neural sensors based on 2D materials

Non-invasive neural interfaces	Application	Contact surface area	On-Skin Contact impedance	Normalized impedance	SNR	Stability tests	Ref
Micro array of rGO on PDMS (e-skin)	EEG, EMG, EOG	N/A	~ 500 kΩ at 50 Hz	N/A	16.8 dB	60 times reuse and 58h stability	82
Laser induced GO on PET	ECG	4 cm^2	~ 60 kΩ at 50 Hz	~240 kΩ.cm^2 at 10 Hz	~70dB	108 h stability	83
graphene on PI	EEG	4 cm^2	~200±10 kΩ at 100 Hz	~800±10 kΩ. cm^2 at 100Hz	N/A	7h stability	84
rGO on nylon membrane	ECG, EMG	N/A	~15 kΩ at 100 Hz	N/A	N/A	52h in testing, 7 days in water	85
CVD graphene/PMMA tattoo	ECG, EMG, EEG, EOG	1.225 cm^2 (0.245 cm2 x 5)	~ 13 kΩ at 1 kHz	~ 15.92 kΩ at 1000 Hz	15.22 dB	N/A	90
Laser scribed Graphene on PU nanomesh	EEG, ECG, EOG	1.5 cm^2	N/A	N/A	14.12 dB	>1000 cycles	93
PEDOT:PSS transferred CVD graphene film	EEG, ECG, EOG, sEMG	N/A	~32 kΩ at 100 Hz	N/A	23 ± 0.7 dB	~12 h stability	94
rGO dip coated nylon textiles	EEG	1.5 cm x 1.5 cm	~ 35 kΩ in 100 Hz	~78.75 kΩ.cm^2 in 100 Hz	N/A	N/A	97
rGO-PEDOT:PSS on nylon lycra textiles	ECG	N/A	~50 kΩ at 100 Hz	N/A	21.6 dB	N/A	101
graphitized electrospun fiber/monolayer graphene into the soft SEBS elastomer	ECG, EEG, sEMG	N/A	N/A	N/A	~ 30 dB	10 repeats	104
Epitaxial graphene on silicon	EEG	1 cm^2	68±4 kΩ at 10 Hz	68±4 kΩ.cm^2 at 10 Hz	N/A	120 days immersed in saline solution	80
Laser-induced porous graphene on silicon elastomer	EEG, ECG, EMG	N/A	≈17 kΩ at 100 Hz	N/A	~ 24.1 dB	10 repeats	123

Ti3C2Tx MXene	EMG	1 cm^2	~ 29.78 ± 8.18 k$\Omega.cm^2$ at 1 kHz	~ 29.78 ± 8.18 k$\Omega.cm^2$ at 1 kHz	~ 39.23 ± 16.25 dB	N/A	125
Mxene 3D mini pillars	EEG, EMG, EOG	N/A	2.8 ± 0.9 kΩ at 1kHz	N/A	N/A	N/A	68
$PtSe_2$ and $PtTe_2$	EMG, ECG, EOG, EMG	N/A	4.94 ± 1.61 kΩ at 10 kHz	N/A	84 ± 6 dB	~ 24 h	128

4.3. Stability in sweat and skin moisture: The *stratum corneum*, or the outermost layer of the epidermis, is usually contaminated with dirt, oils, microbes, and sweat. [134] The sweat generated over time contains physiological salts and can induce corrosion of the electrodes. [135] The graphene oxide-based sensors showed good stability with the presence of sweat for their hydrophilic surface that formed due to the presence of the surface functional groups. [85] The small grains of the epitaxial graphene on SiC/Si contributed to improving the performance with the repeated testing *via* forming a thin layer of water boundary in the presence of sweat and increasing the graphene's hydrophilicity, also simultaneously leading to an enhanced ion intercalation hence an improved contact impedance with the skin. [80] The recently developed MXene-based sensors, due to their surface hydrophilicity and aqueous processability, also demonstrated good stability in water. [68] Another approach to avoid delamination or loose on-skin attachment of hydrophobic graphene due to sweat and skin moisture is to introduce gas permeability or breathability by patterning in an open mesh structure or on a nanoporous membrane. [123, 129]

4.4. Acquiring signals through hair: The vast majority of the reported 2D materials-based sensors, including the sensors listed in table 2, are flat (thin-film) in nature hence more suitable for contact on hairless parts of the body like the forehead and forearm. [130] To control EEG-based robotics with the eyeball movement or visual flickering to oscillate neuron signal, the most appropriate sensor location is the parietal lobes near the back and top of the head. [68, 135] This part of the head is covered with hair with a typical density of 70 to 100 hairs per cm^2 with a single hair diameter of ~80 µm. [136] Among the listed sensors in Table 2, only the MXene-based 3D mini-pillar array sensors has been employed on the hairy portion of the head of a human subject having ~5 mm of hair size. [68] The recordings were made using the MXtrode device containing eight dry 3D mini-pillar electrodes (3 mm in height and 3 mm in diameter) arranged at a distance of 500 µm and one standard Ag/AgCl wet electrode placed in the centre

as reference and ground electrode on the parietal region. This aspect will still require extensive further development of 2D materials electrodes.

The additional functionalities of 2D materials offer the future capability to be used for added redundancy or multipurpose sensing, for example combining the electrochemical-based sensing on which this review was based, with a range of optical biosensing capabilities. [126, 137] In addition, the ability to integrate with electronic circuitry for wireless signal monitoring would be of great value, like in the case of the graphene-based all-printed, nanomembrane hybrid EMG sensor showing hand-gesture-controlled wireless robotic devices, such as drones, RC cars, and bionic arms. [138] Finally, self-powered devices could lead to autonomous systems where the integrated sensing devices harness power from sources like thermoelectric, piezoelectric, and triboelectric generators without needing a battery and can run interruptedly for continuous operation for health monitoring. [139, 140] The integration of these energy-harvesting devices with the neural sensors could enable uninterrupted wireless biopotential signal monitoring for healthcare and to control robotic devices.

5. CONCLUSION

We have reviewed the recent progress of 2D materials-based sensors for both invasive/implantable and non-invasive recording of biopotentials from the brain.

2D materials are of high interest in this area thanks to their extremely thin nature, as well as thanks to the ability of bringing together several functionalities at once, enabling the ultimate miniaturisation of the biosensor system.

The most investigated 2D material for neural electrodes to-date has been graphene by far, with some recent works focusing on the use of TMDs and MXenes. Therefore, while graphene sensing is reaching some level of maturity, neural interfaces based on alternate 2D materials are still at an early stage of development. Detailed studies on cytotoxicity, biocompatibility, stability, and durability are required, particularly for their use as invasive sensors, which have the most stringent requirements.

Regarding non-invasive dry sensors based on 2D materials, we have condensed and compared in Table 2 the main parameters of impedance, signal to noise ratio, repeatability, and durability as published in key recent studies. Most of these parameters still lag behind the Ag/AgCl wet sensors, which are the benchmark sensors but cannot be easily used outside of clinical settings.

However, the recent progress in electrical performance reported in some recent studies creates a reasonable expectation that 2D materials-based sensors could match or do better than wet sensors in the future, also thanks to an improvement of the whole dry sensor systems. Biopotential detection from hairy areas of the head, to detect signals from parietal and occipital lobes of the brain, is still in general a key challenge for thin-film sensors, more than just for 2D materials.

AUTHOR INFORMATION

Corresponding Author

* Francesca Iacopi **-** *School of Electrical and Data Engineering, Faculty of Engineering and Information Technology, University of Technology Sydney, Ultimo NSW, 2007, Australia;*
Email- francesca.iacopi@uts.edu.au

Author

Shaikh Nayeem Faisal- *School of Electrical and Data Engineering, Faculty of Engineering and Information Technology, University of Technology Sydney, Ultimo NSW, 2007, Australia.*

Funding

The authors acknowledge funding from the Defence Innovation Hub, an initiative of the Australian Government, contract P18-650825.

Notes

The authors declare no competing financial interest.

REFERENCES:

(1) Hatspoulos, N. G.; Donoghue, J. P. The science of neural interface systems. *Annu. Rev. Neurosci.* **2009**, *32*, 249-266.

(2) Fattahi, P.; Yang, G.; Kim, G.; Abidian, M. R. A review of organic and inorganic biomaterials for neural interfaces. *Adv. Mater*. **2014**, *26,* 1846-1885.

(3) Zeng, Q.; Li, X.; Zhang, S.; Deng, C.; Wu, T. Think big, see small-A review of nanomaterials for neural interfaces. *Nano Select* **2021**, 1–16.

(4) Casson, A. J. Wearable EEG and beyond, *Biomed. Eng. Lett.* **2019**, *9*, 53-71.

(5) Donoghue, J. P. Connecting cortex to machines: recent advances in brain interfaces. *Nat. Neurosci.* **2002**, *5,* 1085-1088.

(6) Wellman, S. M.; Eles, J. R.; Ludwig, K. A.; Seymour, J. P.; Michelson, N. J.; McFadden, W. E.; Vazquez, A. L.; Kozai, D. Y. A materials roadmap to functional neural interface design. *Adv. Funct. Mater*. **2018**, *28,* 1701269.

(7) Donoghue, J. P. Bridging the brain to the world: A perspective on neural interface systems. *Neuron* **2008**, *60*, 511-521.

(8) Karbowski, K. Electroencephalography, the past and future, *Eur. Neurol*. **1990**, *30*, 170-175.

(9) Tait, L.; Tamagnini, F.; Stothart, G.; Barvas, E.; Monaldini, C.; Frusciante, R.; Volpini, M.; Guttmann, S.; Coulthard, E.; Brown, J. T.; Kazanina, N.; Goodfellow, M. EEG microstate complexity for aiding early diagnosis of Alzheimer's disease. *Sci. Rep.* **2020,** *10*, 17627.

(10) Sharma, N.; Kolekar, M. H.; Chandra, S. The role of EEG signal rocessing in detection of neurocognitive disorders. *Int. J. Behav. Healthcare Res.* **2016**, *6*, 15-27.

(11) Al-Qazzaz, N. K.; Ali, S. H. B. M.; Ahmad, S. A.; Chellappan, K.; Islam, M. S.; Escudero, J. Role of EEG as biomarker in the early detection and classification of dementia. *ScientificWorldJournal* **2014**, *2014*, 906038.

(12) Shaban, M.; Amara, A. W. Resting-state electroencephalography based deep-learning for the detection of Parkinson's disease. *PLoS One* **2022**, *17(2),* e0263159.

(13) Rich, S. I.; Wood, R. J.; Majidi, C. Untethered soft robotics. *Nat. Electron.* **2018**, *1,* 102-112.

(14) Kerous. B.; Skola. F.; Liarokapis F. EEG-based BCI and video games: a progress report. *Virtual Real*. **2018**, *22*, 119-135.

(15) Wang, Y. K.; Chen, S. A.; C. T. Lin, An EEG-based brain-computer interface for dual task driving detection, *Neurocomputing* **2014**, 129, 85-93.

(16) Tudor, M.; Tudor, L.; Tudor, K. I. [Hans Berger (1873-1941)—the history of electroencephalography]. *Acta Med Croatica* **2005**, *59(4),* 307-313.

(17) Spilker, B.; Kamiya, J.; Callaway, E.; Yeager, C. L. Visual Evoked Responses in Subjects Trained to Control Alpha Rhythms. *Psychophysiology* **1969**, *5*, 683-695.

(18) Rezeika, A.; Benda, M.; Stawicki, P.; Gembler, F.; Saboor, A.; Volosyak, I. Brain-computer interface spellers: A review, *Brain. Sci.* **2018**, *8(4),* 57.

(19) Cincotti, F.; Mattia, D.; Aloise, F.; Bufalari, S.; Schalk, G.; Oriolo, G.; Cherubini, A.; Marciani, M. G.; Babiloni, F. Non-Invasive brain-computer interface system: towards its application an assistive technology. *Brain Res. Bull*. **2008**, *75*, 796-803.

(20) Bell, C. J.; Shenoy, P.; Chalodhorn, R.; Rao, P. N. Control of a humanoid robot by a non-invasive brain-computer interface in humans, *J. Neural Eng*. **2008**, *5,* 214.

(21) Penaloza, C. I.; Nishio, S. BMI control of a third arm for multitasking. *Sci. Robot.* **2018,** *3,* 1228.

(22) Parvizi, J.; Kastner, S. Promises and limitations of human intracranial electroencephalography, *Nat. Neurosci.* **2018**, *21*, 474-483.

(23) Song, E.; Li, J.; Won, S. M.; Bai, W.; Rogers, J. A. Materials for flexible bioelectronic systems as chronic neural interfaces. *Nat. Mater.* **2020**, *19,* 590-603.

(24) Lopez-Gordo, M. A.; Sanchez-Morillo, D.; Valle, F. P. Dry EEG electrodes. *Sensors* **2014**, *14(7),* 12847-12870.

(25) Spüler, M. A high-speed brain-computer interface (BCI) using dry EEG electrodes. *PLoS One* **2017,** *12(2),* e0172400.

(26) Li, G. L.; Wu, J. -T.; Xia, Y. -H.; He, Q. -G.; Jin, H. -G. Review of semi-dry electrodes for EEG recording. *J Neural Eng.* **2020,** *17,* 051004.

(27) Sheng, X.; Qin, Z.; Xu, H.; Shu, X.; Gu, G.; Zhu, X. Soft ionic-hydrogel electrodes for electroencephalography signal recording. *Sci. China Technol. Sci.* **2021,** *64,* 273-282.

(28) Oldroyd, P.; Malliaras, G. G. Achieving long-term stability of thin-film electrodes for neurostimulation. *Acta Biomater*. **2021**, *139*, 65-81.

(29) LaRocco, J.; Le, M. D.; Paeng, D. -G. A systemic review of available low-cost EEG headsets used for drowsiness detection. *Front. Neuroinform*. **2020,** *14*, 553352.

(30) Geim, A. K.; Novoselov, K. S. The rise of graphene. *Nat. Mater*. **2007,** *6*, 183-191.

(31) Gogotsi, Y.; Anasori, B. The rise of MXenes. ACS Nano 2019, 13 (8), 8491-8494.

(32) Katzmarek, D.; Pradeepkumar, A.; Ziolkowski, R.; Iacopi, F. Review of graphene for the generation, manipulation, and detection of electromagnetic fields from microwave to terahertz. *2D Mater*. **2022**, *9*, 022002.

(33) Schaefer, N.; Gracia-Cortadella, R.; Calia, A. B.; Mavredakis, N.; Illa, X.; Masvidal-Codina, E.; Cruz, J.; Corro, E.; Rodríguez, L.; Prats-Alfonso, E.; Bousquet, J.; Martínez-Aguilar, J.; Pérez-Marín, A. P.; Hébert, C.; Villa, R.; Jiménez, D.; Guimerà-Brunet, A.; Garrido, J. A. Improved metal-graphene contacts for low-noise, high-density microtransistor arrays for neural sensing. *Carbon* **2020**, *161*, 647-655.

(34) Chiang, C. -H.; Wang, C.; Barth, K.; Rahimpour, S.; Trumpis, M.; Duraivel, S.; Rachinskiy, I.; Dubey, A.; Wingel, K. E.; Wong, M.; Witham, N. S.; Odell, T.; Woods, V.; Bent, B.; Doyle, W.; Friedman, D.; Bihler, E.; Reiche, C. F.; Southwell, D. G.; Haglund, M. M.; Friedman, A. H.; Lad, S. P.; Devore, S.; Devinsky, O.; Solzbacher, F.; Pesaran, B.; Cogan, G. Viventi, J. Flexible, high-resolution thin-film electrode for human and animal neural research, *J Neural Eng.* **2021,** *18*, 045009.

(35) Manzeli, S.; Ovchinnikov, D.; Pasquier, D.; Yazyev, O. V.; Kis, A. 2D transition metal dichalcogenides. *Nat. Rev. Mater*. **2017**, *2*, 17033.

(36) Liu, Y.; Feig, V. R.; Bao, Z. Conjugated polymer for implantable electronics toward clinical application. *Adv. Healthcare Mater*. **2021,** *10,* 2001916.

(37) Jun, J. J.; Steinmetz, N. A.; Siegle, J. H.; Denman, D. J.; Bauza, M.; Barbarits, B.; Lee, A. K.; Anastassiou, C. A.; Andei, A.; Aydin, C.; Barbic, M.; Blanche, T. J.; Bonin, V.; Couto, J.; Dutta, B.; Gratiy, S. L.; Gutnisky, D. A.; Häusser, M.; Karsh, B.; Ledochowitsch, P.; Lopez, C. M.; Mitelut, C.; Musa, S.; Okun, M.; Pachitariu, M.; Putzeys, J.; Rich, P. D.; Rossant, C.; Sun, W. L.; Svoboda, K.; Carandini, M.; Harris, K. D.; Koch, C.; O'Keefe, J.; Harris, T. D. Fully integrated silicon probes for high-density recording of neural activity. *Nature* **2017,** *551*, 232-236.

(38) Musk, E. An integrated brain-machine interface platform with thousands of channels, *J. Med. Internet Res*. **2019**, *21*, e16194.

(39) Choi, J.; Kim, S. -M.; Ryu, R. -H.; Kim, S. -P.; Sohn, J. -W. Implantable neural probes for brain-machine interfaces-current developments and future prospects. *Exp. Neurobiol*, **2018**, *27(6)*, 453-471.

(40) Alahi, M. E. E.; Liu, Y.; Xu, Z.; Wang, H.; Wu, T.; Mukhopadhyay, S. C. Recent advancement of electrocorticography (ECoG) electrodes for chronic neural recording/stimulation. *Mater. Today Commun.* **2021**, *29*, 102853.

(41) Won, S. M.; Song, E.; Zhao, J.; Li, J.; Rivnay, J.; Rogers, J. A. Recent Advances in Materials, Devices, and Systems for Neural Interfaces. *Adv. Mater.* **2018,** *30,* 1800534.

(42) Yan, R.; Park, J. -H.; Choi, Y.; Heo, C. -J.; Yang, S. -M.; Lee, L. P.; Yang, P. Nanowire-based single-cell endoscopy. *Nat. Nanotechnol.* **2012,** *7,* 191-196.

(43) Lu, Y.; Lyu, H.; Richardson, A. G.; Lucas, T. H.; Kuzum, D. Flexible neural electrode array based-on porous graphene for cortical microstimulation and sensing. *Sci. Rep.* **2016**, *6*, 33526.

(44) Veronica, A.; Li, Y.; Hsing, I. Minimally invasive & long-lasting neural probes from a materials perspective. *Electroanalysis* **2019**, *31(4),* 586-602.

(45) Kostarelos, K.; Vincent, M.; Hebert, C.; Garrido, J. A. Graphene in the design and engineering of next-generation interfaces. *Adv. Mater.* **2017**, *29,* 1700909.

(46) Lu, Y.; Kuzum, D. Graphene-based neurotechnologies for advanced neural interfaces. *Curr. Opin. Biomed. Eng.* **2018,** *6,* 138-147.

(47) Xu, B.; Pei, J.; Feng, L.; Zhang, X. -D. Graphene and graphene-related materials as brain electrode. *J Mater Chem B* **2021**, *9,* 9485-9496.

(48) Fairfield, J. A. Nanostructured materials for neural electrical interfaces, *Adv. Funct. Mater.* **2018**, *28*, 1701145.

(49) Kuzum, D.; Takano, H.; Shim, E.; Reed, J. C.; Juul, H.; Richardson, A. G.; Vries, J. D.; Bink, H.; Dichter, M. A.; Lucas, T. H.; Coulter, D. A.; Cubukcu, E.; Litt, B. Transparent and flexible low noise graphene electrodes for simultaneous electrophysiology and neuroimaging. *Nat. Commun.* **2014**, *5*, 5259.

(50) Wang, K.; Frewin, C. L.; Esrafilzadeh, D.; Yu, C.; Wang, C.; Pancrazio, J. J.; Romero-Ortega, M.; Jalili, R.; Wallace, G. High-performance graphene-fiber based neural recording microelectrodes, *Adv. Mater.* **2019,** *31*, 1805867.

(51) Fang, B.; Chang, D.; Xu, Z.; Gao, C. A review on graphene fibers: expectations, advances, and prospects. *Adv. Mater.* **2020**, *32 (5),* 1902664.

(52) Xu, T.; Zhang, Z.; Qu, L. Graphene-based fibers: recent advances in preparation and application. *Adv. Mater.* **2020,** *32 (5),* 1901979.

(53) Gracia-Cortadella, R.; Schäfer, N.; Cisneros-Fernandez, J.; Ré L.; Illa, X.; Schwesig, G.; Moya, A.; Santiago, S.; Guirado, G.; Villa, R.; Sirota, A.; Serra-Graells, F.; Garrido, J. A.; Guimerà-Brunet, A. Switchless multiplexing of graphene active sensor arrays for brain mapping. *Nano Lett.* **2020,** *20 (5),* 3528-3537.

(54) Masvidal-Codina, E.;Illa, X.; Dasliva, M.; Calia, A. B.; Dragojević, Vidal-Rosas, E. E.; Prats-Alfonso, E.; Martinez-Aguilar, J..; Cruz, J. M. D. L.; Garcia-Cortadella, R.;Godignon, P.; Rius, G.; Camassa, A.; Corro, E. D.; Bousquet, J.; Hebert, C.; Durduran, T.; Villa, R.; Sanchez-Vives, M. V.; Garrido, J. A.; Guimerà-Brunet, A. High-resolution mapping of infraslow cortical brain activity enabled by graphene microtransistors, *Nat. Mater*. **2019**, *18*, 280-288.

(55) Garcia-Cortadella, R.; Schwesig, G.; Jeschke, C.; Illa, X.; Gray, A. L.; Savage, S.; Stamatidou, E.; Schiessl, I.; Masvidal-Codina, E.; Kostrelos, A.; Guimerà-Brunet, A.; Sirota, A.; Garrido, J. A. Graphene active sensor arrays for long-term and wirelessly mapping of wide frequency band epicortical brain activity. *Nat. Commun*. **2021**, *12,* 211.

(56) Park, D. -W.; Schendel, A. A.; Mikael, S.; Brodnick, S. K.; Richner, T. J.; Ness, J. P.; Hayat, M. R.; Atry, F.; Frye, S. T.; Pashaie, R.; Thongpang, S.; Ma, Z.; Williams, J. C. Graphene-based carbon-layered electrode array technology for neural imaging and optogenetic applications. *Nat. Commun.* **2014**, *5,* 5258.

(57) Thnermann, M.; Lu, Y.; Liu, X.; Kilic, K.; Desjardins, M.; Vandenberghe, M.; Sadegh, S.; Saisan, P. A.; Cheng, Q.; Weldy, K. L.; Lyu, H.; Djurovic, S.; Andreassen, O. A.; Dale, A. M.; Devor, A.; Kuzum, D. Deep 2-photon imaging and artefact-free optogentics through transparent graphene microelectrode arrays. *Nat. Commun* **2018**, *9*, 2035.

(58) Lu, Y.; Liu, X.; Hattori, R.; Ren, C.; Zhang, X.; Komiyama, T.; Kuzum, D. Ultrolow impedance graphene microelectrodes with high optical transparency for simultaneous deep two-photon imaging in transgenic mice. *Adv. Funct. Mater*. **2018**, *28 (31),* 1800002.

(59) Calia, A. B.; Masvidal-Codina, E.; Smith, T. M.; Schäfer, N.; Rathore, D.; Rodríguez-Lucas, E.; Illa, X.; Cruz, J. M. D.; Corro, E. D.; Prats-Alfonso, E.; Viana, D.; Bousquet, J.; Hébert, C.; Martínez-Aguilar, J.; Sperling, J. R.; Drummond, M.; Halder, A.; Dodd, A.; Barr, A.; Barr, K.; Savage, S.; Fornell, J.; Sort, J.; Guger, C.; Villa, R.; Kostarelos, K.; Wykes, R. C.; Guimerà-Brunet, A.; Garrido, J. A. Full-bandwidth electrophysiology of seizures and epileptiform activity enabled by flexible graphene microtransistor depth neural probes. *Nat. Nanotechnol*. **2022**, *17*, 301-309.

(60) Pradeepkumar, A.; Amjadipour, M.; Mishra, N.; Liu, C.; Fuhrer, M. S.; Bendavid,A.; Isa, F.; Zielinski, M.; Sirikumara, H. I.; Jayasekara, T.; Gaskill, D. K.;

Iacopi, F. P-type epitaxial graphene on cubic silicon carbide on silicon for integrated silicon technologies. *ACS Appl. Nano Mater.* **2020**, *3(1),* 830-841.

(61) Islam, M. M.; Faisal, S. N.; Akhter, T.; Roy, A. K.; Minett, A. I.; Konstantinov, K.; Dou, S. X. Liquid-crystal-mediated 3D macrostructured composite Co/Co3O4 embedded in graphene: Free-standing electrode for efficient water splitting. *Part. Part. Syst. Charac.* **2017**, *34*, 1600386.

(62) Islam, M. S.; Faisal, S. N.; Tong, L.; Roy, A. K.; Zhang, J.; Haque, E.; Minett, A. I.; Wang, C. H. N-doped reduced graphene oxide (rGO) wrapped carbon microfibers as binder-free electrodes for flexible fibre supercapacitors and sodium-ion batteries. *J Energy Storage* **2021**, *37*, 102453.

(63) Halim, A.; Qu, K. -Y.; Zhang, X. -F.; Huang, N. -P.; Recent advances in the application of two-dimensional nanomaterials for neural tissue engineering and regeneration, *ACS Biomater. Sci. Eng.* **2021**, *7*, 3503-3529.

(64) Murali, A.; Lokhande, G.; Deo, K. A.; Brokesh, A.; Gaharwar, A. K.; Emerging 2D nanomaterials for biomedical applications, *Mater. Today* **2021**, *50,* 276-302.

(65) Choi, C.; Choi, M. K.; Liu, S.; Kim, M. S.; Park, O. K.; Im, C.; Kim, J.; Qin, X.; Lee, G. J.; Cho, K. W.; Kim, M.; Joh, E.; Lee, J.; Son, D.; Kwon, S. -H.; Jeon, N. L.; Song, Y. M.; Lu, N.; Kim, D. -H. Human eye-inspired soft optoelectronic device using high-density MoS_2-graphene curved image sensor array, *Nat. Commun*. **2017**, *8*, 1664.

(66) Huang, J.; Li, Z.; Mao, Y.; Li, Z. Progress and biomedical applications of MXenes. *Nano Select* **2021**, *2 (8),* 1480-1508.

(67) Driscoll, N.; Richardson,A. G.; Maleski, K.; Ansori, B.; Adewole, O.; Lelyukh, P.; Escobedo, L.; Cullen, D. K.; Lucas, T. H.; Gogotsi, Y.; Vitale, F. Two-dimensional Ti_3C_2 MXene for high-resolution neural interfaces. *ACS Nano* **2018**, *12 (10),* 10419-10429.

(68) Driscoll, N.; Erickson, B.; Murphy, B. B.; Richardson, A. G.; Robbins, G.; Apollo, N. V.; Mentzelopoulos, G.; Mathis, T,; Hantanasirisakul, K.; Bagga, P.; Gullbrand, S. E.; Sergison, M.; Reddy, R.; Wolf, J. A.; Chen, H. I.; Lucas, T. H.; Dillingham, T. R.; Davis, K. A.; Gogotsi, Y.; Medaglia, J. D.; Vitale, F. MXene-infused bioelectronic interfaces for multiscale electrophysiology and stimulation. *Sci. Trans. Med.* **2021**, *13,* 612.

(69) Lim, G. P.; Soon, C. F.; Ma, N. L.; Morsin, M.; Nayan, N.; Ahmad, M. K.; Tee, K. S. Cytotoxicity of MXene-based nanomaterials for biomedical applications: A mini review. *Environ. Res.* **2021**, *201*, 111592.

(70) Wu, W.; Ge, H.; Zhang, L.; Lei, X.; Yang, Y.; Fu, Y.; Feng, H. Evaluating the cytotoxicity of Ti_3C_2 MXene to neural stem cells. *Chem. Res. Toxicol.* **2020**, *33 (12),* 2953-2962.

(71) Zhang, J.; Fu, Y.; Mo, A. Multilayered titanium carbide MXene film for guided bone regeneration. *Int J Nanomedicine* **2019,** *14,* 10091-10103.

(72) Sundaram, A.; Ponraj, J. S.; Wang, C.; Peng, W. K.; Manavalan, R. K.; Dhanabalan, S. C.; Zhang, H.; Gaspar, J. Engineering of 2D transition metal carbides and nitrides MXenes for cancer therapeutics and diagnostics. *J Mater. Chem B* **2020,** *8,* 4990-5013.

(73) Yu, J.; Yang, X.; Gao, G.; Xiong, Y.; Wang, Y.; Han, J.; Chen, Y.; Zhang, H.; Sun, Q.; Wang, Z. L. Bioinspired mechano-photonic artificial synapse based on graphene/ MoS2 heterostructure. *Sci. Adv.* **2021,** *7*, 9117.

(74) Barua, S.; Dutta, H. S.; Gogoi, S.; Devi, R.; Khan, R. Nanostructured MoS_2-based advanced biosensors: A review. *ACS Appl. Nano Mater.* **2018**, *1 (1),* 2-25.

(75) Yadav, V.; Roy, S.; Singh, P.; Khan, Z.; Jaiswal, A. 2D MoS_2-based nanomaterials for therapeutic, bioimaging and biosensing applications. *Small* **2019**, *15 (1),* 1803706.

(76) Gong, L.; Feng, L.; Zheng, Y.; Luo, Y.; Zhu, D.; Chao, J.; Su, S.; Wang, L. Molybdenum disulphide-based nanoprobes: Preparation and sensing applications. *Biosensors* **2022**, *12 (2),* 87.

(77) Appel, J. H.; Li, D. O.; Podlevsky, J. D.; Debnath, A.; Green, A. A.; Wang, Q. H.; Chae, J. Low cytotoxicity and genotoxicity of two-dimensional MoS_2 and WS_2. *ACS Biomater. Sci. Eng.* **2016**, *2, 3*, 361-367.

(78) Radhakrishnan, S. S.; Sebastian, A.; Oberoi, A.; Das, S.; Das, S. A biomimetic neural encoder for spiking neural network. *Nat. Commun.* **2021**, *12*, 2143.

(79) Chen, X.; Park, Y. J.; Kang, M.; Kang, S. -K.; Koo, J.; Shinde, S. M.; Shin, J.; Jeon, S.; Park, G.; Yan, Y.; MacEwan, M. R.; Ray, W. Z.; Lee, K. -M.; Rogers, J. A.;

Ahn, J. -H. CVD-grown monolayer MoS_2 in bioabsorbable electronics and biosensors. *Nat. Commun.* **2018**, *9,* 1690.

(80) Faisal, S. N.; Amjadipour, M.; Izzo, K.; Singer, J. A.; Bendavid, A.; Lin, C. -T.; Iacopi, F. Non-invasive on-skin sensors for brain machine interfaces with epitaxial graphene. *J. Neural Eng*. **2021,** *18,* 066035.

(81) Jung, J. M.; Cha, D. Y.; Kim, D. S.; Yang, H. J.; Choi, K. S.; Choi, J. M.; Chang, S. P. Development of PDMS-based Flexible dry type SEMG electrodes by micromachining technologies. *Appl. Phys. A* **2014**, *116*, 1395-1401.

(82) Li, Z.; Guo, W.; Huang, Y.; Zhu, K.; Yi, H.; Wu, H. On-skin graphene electrodes for large area electrophysiological monitoring and human-machine interfaces. *Carbon* **2020**, *164*, 164-170.

(83) Murastaov, G.; Bogatova, E.; Brazovskiy, K.; Amin, I.; Lipovka, A.; Dogadina, E.; Cherepnyov, A.; Ananyeva, A.; Plonikov, E.; Ryabov, V.; Rodriguez, R. D.; Sheremet, E. Flexible and water-stable graphene-based electrodes for long-term use in bioelectronics. *Biosens. Bioelectron*. **2020**, *166,* 112426-112436.

(84) Kim, H.; Kwon, S.; Kwon, Y. -T.; Yeo, W. -H. Soft wireless bioelectronics and differential electrodermal activity for home sleep monitoring. *Sensors* **2021**, *21(2),* 354.

(85) Das, P. S.; Park, S. H.; Baik, K. Y.; Lee, J. W.; Park, J. Y. Thermally reduced graphene oxide-nylon membrane based epidermal sensor using vacuum filtration for wearable electrophysiological signals and human motion monitoring. *Carbon* **2020,** *158,* 386-393.

(86) Islam, M. R.; Afroz, S.; Beach, C.; Islam, M. H.; Parraman, C.; Abdelkader, A.; Casson, A. J.; Novoselove, K. S.; Karim, N. Fully printed and multifunctional graphene-based wearable e-textiles for personalized healthcare applications. *iScience* **2022**, 103945.

(87) Wang, B.; Facchetti, A.; Mechanically flexible conductors for stretchable and wearable e-Skin and e-Textile devices. *Adv. Mater.* **2019**, *31 (28),* 1901408.

(88) Sanderson, K. Electronic skin: from flexibility to a sense of touch, *Nature* **2021,** *591*, 685-687.

(89) Yang, J. C.; Mun, J.; Kwon, S. Y.; Park, S.; Bao, S.; Park, S. Electronic skin: recent progress and future prospects for skin-attachable devices for health monitoring, robotics, and prosthetics. *Adv. Mater*. **2019**, *31 (48),* 1904765.

(90) Ameri, S. K.; Ho, R.; Jang, H.; Tao, L.; Wang, Y.; Wang, L.; Schnyer, D. M.; Akinwande, D.; Lu, N. Graphene electronic tattoo sensors. *ACS Nano* **2017**, *11 (8),* 7634-7641.

(91) Ameri, S. K.; Kim, M.; Kuang, I. A.; Perera, W. K.; Alshiekh, M.; Jeong, H.; Topcu, U.; Akinwande, D.; Lu, N. Imperceptible electrooculography graphene sensor system for human-robot interface. *NPJ 2D Mater. Appl.* **2018**, *2,* 19.

(92) Kireev, D.; Ameri, S. K.; Nederveld, A.; Kampfe, J.; Jang, H.; Lu, N.; Akinwande, D. Fabrication, characterization and application of graphene electronic tattoos. *Nat. Protoc.* **2021**, *16,* 2395-2417.

(93) Qiao, Y.; Li, X.; Wang, J.; Ji, S.; Hirtz, T.; Tian, H.; Jian, J.; Cui, T.; Dong, Y.; Xu, X.; Wang, F.; Wang, H.; Zhou, J.; Yang, Y.; Someya, T. Ren, T. -L. Intelligent and multifunctional graphene nanomesh electronic skin with high comfort, *Small* **2022,** *18* (7), 2104810.

(94) Zhao, Y.; Zhang, S.; Yu, T.; Zhang, Y.; Ye, G.; Cui, H.; He, C.; Jiang, W.; Zhai, Y.; Lu, C.; Gu, X.; Liu, N. Ultra-conformal skin electrodes with synergistically enhanced conductivity for long-time and low-motion artifact epidermal electrophysiology. *Nat. Commun*. **2021**, *12,* 4880.

(95) Golparvar, A. J.; Yapici, M. K. Electrooculography by wearable graphene textile. *IEE Sensors* **2018**, *18,* 8971 – 8978.

(96) Afroz, S.; Karim, N.; Wang, Z.; Tan, S.; He, P.; Holwill, M.; Ghazaryan, D.; Fernanado, A.; Novoselov, K. S. Engineering graphene flakes for wearable textile sensors via highly scalable and ultrafast yarn dyeing technique. *ACS Nano* **2019,** *13 (4),* 3847-3857.

(97) Golparvar, A.; Ozturk, O.; Yapici, M. K. Gel-free wearable electroencephalography (EEG) with soft graphene textiles. *IEEE Sensors* **2021,** *doi:10.1109/SENSORS47087.2021.9639711.*

(98) Ba, H.; Truong-Phuc, L.; Papaefthimiou, V.; Sutter, S.; Pronkin, S.; Bahouka, A.; Lafue, Y.; Nguyen-Dinh, L.; Giambastiani, G.; Pham-Huu, C. Cotton fabrics coated with few-layer graphene as highly responsive surface heaters and integrated lightweight electronic-textile circuits. *ACS Appl. Nano Mater*. **2020**, *3(10),* 9771-9783.

(99) Shuvo, I. I.; Shah, A.; Dagdeviren, C.; Electronic textile sensors for decoding vital body signals: state-of-the-art review on characterizations and recommendations, *Adv. Intelligent Syst.* **2022,** 2100223.

(100) Shathi, M. A.; Minzhi, C.; Khoso, N. A.; Deb, H.; Ahmed, A.; Sai, W. S. All organic graphene oxide and Poly(3,4-ethylene dioxythiophene)-Poly (styrene sulfonate) coated knitted textile fabrics for wearable electrocardiography (ECG). *Synth. Met.* **2020**, *263*, 116329.

(101) Shathi, M. A.; Chen, M.; Khoso, N. A.; Rahman, M. T.; Bhattacharjee, B. Graphene coated textile based highly flexible and washable sports bra for human health monitoring. *Mater. Des.* **2020**, *193*, 108792.

(102) Wang, Y.; Yokota, T.; Someya, T. Electrospun nanofiber-based soft electronics. *NPG Asia Mater.* **2021**, *13*, 22.

(103) Hu, Q.; Nag, A.; Xu, Y.; Han, T.; Zhang, L. Use of graphene-based fabric sensors for monitoring human activities. *Sens. Actuators, A: Physical* **2021,** *332,* 113172.

(104) Qiu, J.; Yu, T.; Zhang, W.; Zhao, Z.; Zhang, Y.; Ye, G.; Zhao, Y.; Du, X.; Liu, X.; Yang, L.; Zhang, L.; Qi, S.; Tan, Q.; Guo, X.; Li, G.; Guo, S.; Sun, H.; Wei, D.; Li, N. A bioinspired, durable, and nondisposable transparent graphene skin electrode for electrophysiological signal detection. *ACS Mater. Lett.* **2020**, *2*, 999-1007.

(105) Xu, Y.; Hu, X.; Kundu, S.; Nag, A.; Afsarimanesh, N.; Sapra, S.; Mukhopadhyay, S. C.; Han, T. Silicon-based sensors for biomedical applications: A review. *Sensors* **2019,** *19(13),* 2908.

(106) Oliveros, A.; Guiseppi-Elie, A.; Saddow, S. E. Silicon carbide: A versatile material for biosensor applications. *Biomed. Microdevices* **2013**, *15,* 353-368.

(107) Bernardin, K.; Frewin, C. L.; Everly, R.; Hassan, J. U.; Saddow, S. E. Demonstration of a robust all-silicon-carbide intracortical neural interface. *Micromachines* **2018,** *9(8)*, 412-430.

(108) Strupinskim W.; Grodecki, K.; Wysmolek, A.; Stepniewski, R.; Szkopek, T.; Gaskell, P. E.; Grüneis, A.; Haberer, D.; Bozek, R.; Krupka, J.; Baranowski, J. M. Graphene epitaxy by chemical vapor deposition on SiC. *Nano Lett.* **2011,** *11 (4),* 1786-1791.

(109) Norimatsu, W.; Kusunoki, M. Epitaxial graphene on SiC{0001}: Advances and perspective. *Phys. Chem. Chem. Phys*. **2014,** *16,* 3501-3511.

(110) Iacopi, F.; Mishra, N.; Cunning, B. V.; Goding, D.; Dimitrijev, S.; Brock, R.; Dauskardt, R. H.; Wood, B.; Boeckl, J. A catalytic alloy approach for graphene on epitaxial SiC on silicon wafers. *J. Mater. Res.* **2015**, *30(5),* 609-615.

(111) Mishra, N.; Boeckl, J. J.; Tadich, A.; Jones, R. T.; Pigram, P. J.; Edmonds, M.; Fuhrer, M. S.; Nichols, B. M.; Iacopi, F. Solid source growth of graphene with Ni–Cu catalysts: Towards high quality in situ graphene on silicon. *J. Phys. D Appl. Phys.* **2017,** *50(9),* 095302.

(112) Cunning, B. V.; Ahmed, M.; Mishra, N.; Kermany, A. R.; Wood, B.; Iacopi, F. Graphitized silicon carbide microbeams: wafer-level, self-aligned graphene on silicon wafers. *Nanotechnology* **2014**, *25(32)*, 325301.

(113) Mishra, N.; Boeckl, J.; Motta, N.; Iacopi, F. Graphene growth on silicon carbide: a review. *Physica Status Solidi (a)* **2016**, *213(9),* 2277-2289.

(114) Pradeepkumar, A.; Amjadipour, M.; Mishra, N.; Liu, C.; Fuhrer, M. S.; Bendavid, A.; Isa, F.; Zielinski, M.; Sirikumara, H. I.; Jayasekara, T.; Gaskill, D. K.; Iacopi, F. P-type epitaxial graphene on cubic silicon carbide on silicon for integrated silicon technologies. *ACS Appl. Nano Mater*. **2020**, *3(1),* 830-841.

(115) Ahmed, M.; Wang, B.; Gupta, B.; Boeckl, J. J.; Motta, N.; Iacopi, F. 2017 On-silicon supercapacitors with enhanced storage performance. *J. Electrochem. Soc.* **2017,** *164(4),* A638.

(116) Amjadpour, M.; Su, D.; Iacopi, F. Graphitic-based solid-state supercapacitors: enabling redox reaction by in situ electrochemical treatment. *Batteries Supercaps*. **2020**, *3(7)*, 587-595.

(117) Mishra, N.; Jiao, S.; Mondal, A.; Khan, Z.; Boeckl, J. J.; Gaskill, K. D.; Brock, R. E.; Dauskardt, R. H.; Iacopi, F. A graphene platform on silicon for the internet of everything. *IEEE 2nd Electron Devices Technology and Manufacturing Conference (EDTM)*, **2018,** 211– 213.

(118) Pang, Y.; Yang, Z.; Yang, Y.; Ren, T. -L. Wearable electronics based on 2D materials for human physiological information detection. *Small* **2020**, *16 (15),* 1901124.

(119) Pradeepkumar, A.; Zielinski, M.; Bosi, M.; Verzellesi, G.; Gaskill, D. K.; Iacopi, F. Electrical leakage phenomenon in heteroepitaxial cubic silicon carbide on silicon. *J Appl Physics* **2018,** *123*, 215103.

(120) Garg, R.; Rastogi, S. K.; Lamparski, M.; Barrera, S. C.; Pace, G. T.; Nuhfer, N. T.; Hunt, B. M.; Meunier, V.; Cohen-Karni, T. Nanowire-mesh-templated growth of out-of-plane three-dimensional fuzzy graphene. *ACS Nano* **2017**, *11(*6), 6301-6311.

(121) Garg, R.; Gopalan, D. P.; Barrera, S. C.; Hafiz, H.; Nuhfer, N. T.; Viswanathan, V.; Hunt, B. M.; Cohen-Karni, T. Electron transport in multidimensional fuzzy graphene nanostructures. *Nano Lett.* **2019**, *19 (8)*, 5335-5339.

(122) Rastogi, S. K.; Bliley, J.; Matino, L.; Garg, R.; Santoro, F.; Feinberg, A. W.; Cohen-Karni, T. Three-dimensional fuzzy graphene ultra-microelectrodes for subcellular electrical recordings. *Nano Res.* **2020**, *13*, 1444-1452.

(123) Sun, B.; McCay, R. N.; Goswami, S.; Xu, Y.; Zhang, C.; Ling, Y.; Lin, J.; Yan, Z. Gas-permeable, multifunctional on-skin electronics based on laser-induced porous graphene and sugar-templated elastomer sponges. *Adv. Mater.* **2018**, *30*, 1804327.

(124) Peng, H. -L.; Sun, Y. -L.; Bi, C.; Li, Q. -F. Development of flexible dry electrode based MXene with low contact impedance for biopotential recording, *Measurement* **2022**, *190*, 110782.

(125) Murphy, B. B.; Mulcahey, P. J.; Driscoll, N.; Richardson, A. G.; Robbins, G. T.; Apollo, N. V.; Maleski, K.; Lucas, T. H.; Gogotsi, Y.; Dillingham, T.; Vitale, F. A gel-free Ti3C2Tx-based electrode array for high-density, high-resolution surface electromyography, *Adv. Mater. Technol*. **2020**, *5 (8),* 2000325.

(126) Tyagi, D.; Wang, H.; Huang, W.; Hu, L.; Tang, Y.; Guo, Z.; Ouyang, Z.; Zhang, H. Recent advances in two-dimensional material based sensing technology toward health and environmental monitoring applications. *Nanoscale* **2020**, *12*, 3535-3559.

(127) Zheng, L.; Wang, X.; Jiang, H.; Xu, M.; Huang, W.; Liu, Z. Recent progress of flexible electronics by 2D transition metal dichalcogenides. *Nano Res.* **2022**, *15,* 2413-2432.

(128) Kireev, D.; Okogbue, E.; Jayanth, R.; Ko, T. -J.; Jung, Y.; Akinwande, D. Multipurpose and reusable ultrathin electronic tattoos based on $PtSe_2$ and $PtTe_2$. *ACS Nano* **2021**, *15 (2),* 2800-2811.

(129) Yan, Z.; Xu, D.; Lin, Z.; Wang, P.; Cao, B.; Ren, H.; Song, F.; Wan, C.; Wang, L.; Zhou, J.; Zhao, X.; Chen, J.; Huang, Y.; Duan, X. Highly stretchable van der Waals thin films for adaptable and breathable electronic membranes. *Science* **2022***, 375*, 852-859.

(130) Yang, L.; Liu, Q.; Zhang, Z.; Gan, L.; Zhang, Y.; Wu, J. Materials for dry electrodes for the electroencephalography: advances, challenges, perspectives. *Adv. Mater. Technol.* **2021**, *7(3),* 2100612.

(131) Albulbul, A. Evaluating major electrodes types for idle biological signal measurements for modern medical technology. *Bioengineering* **2016**, *3*, 20.

(132) Suarez-Perez, A.; Gabriel, G.; Rebollo, B.; Illa, X.; Guimerà-Brunet, A.; Hernádez-Ferrer, J.; Martínez, M. T.; Villa, R.; Sanchez-Vives, M. V. Quantification of signal-to-noise ratio in cerebral cortex recordings using flexible MEAs with co-localized platinum black, carbon nanotubes, and gold electrodes. *Front. Nerosci.* **2018**, *12,* 862.

(133) Norton, J. J. S.; Lee, D. S.; Lee, J. W.; Lee, W.; Kwon, O.; Jung, S. -Y.; Cheng, H.; Jeong, J. -W.; Akce, A.; Umunna, S.; Na, I.; Kwon, Y. H.; Wang, X. -Q.; Liu, Z.; Paik, U.; Huang, Y.; Bretl, T.; Yeo, W. -H.; Rogers, J. A. Soft, curved electrode systems capable of integration on the auricle as a persistent brain-computer interface. *Proc. Natl. Acad. Sci.***2015,** *112 (13),* 3920-3925.

(134) Grice, E. A.; Segre, J. A. The skin microbiome. *Nat. Rev. Microbiol*. **2011**, *9,* 244-253.

(135) Lin, C. T.; King, J. T.; John, A. R.; Huang, K. C.; Cao, Z.; Wang, Y. K. The impact of vigorous cycling exercise on visual attention: a study with the BR8 wireless dry EEG system. *Front. Neurosci*. **2021**, *15*, 621365.

(136) Loussouarn, G.; Lozano, I.; Panhard, S.; Collaudin, C.; Rawadi, C. E.; Genain, G. Diversity in human hair growth, diameter, colour and shape. An *in vivo* study on young adults from 24 different ethnic groups observed in the five continents. *Europ. J. Dermatol.* **2016,** *26,* 144-154.

(137) Lei, Z. -L.; Guo, B. 2D Material-based optical biosensor: status and prospect. *Adv. Sci.* **2022,** *9 (4),* 2102924.

(138) Kwon, Y. -T.; Kim, Y. -S.; Kwon, S.; Mahmood, M.; Lim, H. -R.; Parl, S. -W.; Kang, S. -O.; Choi, J. J.; Herbert, R.; Jang, Y. C.; Choa, Y. -H.; Yeo, W. -H. All-printed nanomembrane wireless bioelectronics using a biocompatible solderable graphene for multimodal human-machine interfaces. *Nat. Commun.* **2020**, *11*, 3450.

(139) Núñez, C. G.; Manjakkal, L.; Dahiya, R. Energy autonomous electronic skin, *NPJ Flex. Electron*. **2019**, *3,* 1.

(140) Liu, Y.; Zhang, S.; Zhou, Y.; Buckingham, M. A.; Aldous, L.; Sherrell, P. C.; Wallace, G. G.; Ryder, G.; Faisal, S.; Officer, D. L.; Beirne, S.; Chen, J. Advanced wearable thermocells for body heat harvesting. *Adv. Energy Mater*. **2020**, *10,* 2002539.